Nonlinear control of an induction motor taking into account saturation and rotor resistance variation effects

Mustapha Es-Semyhy, Abdellfattah Ba-Razzouk, Mustapha El Haroussi, Mhamed Madark
Mathematics, Computer and Engineering Sciences Laboratory, Systems Analysis and Information Processing Team,
Faculty of Science and Technology, Hassan 1st University, Settat, Morocco

Article Info

ABSTRACT

Nowadays, electrical drives require more and more precision and reliability. Induction machine is one of the most robust actuators in terms of maintenance and reliability. Their control requires a good knowledge of the physical phenomena governing its operation. Saturation and heating are two main phenomena that must be taken into account to achieve the desired performance. In this paper, we will synthesize a nonlinear control law based on the "Backstepping" method, to regulate rotor speed and flux. This law takes into account saturation and rotor resistance variation effects. The immunity of the control to temperature rise will be tested. This control strategy is studied by simulation in the MATLAB/Simulink environment.

Corresponding Author:

Mustapha Es-Semyhy
Department of Applied Physics Faculty Science and Technology, Hassan 1st University
Settat, Morocco
Email: mustaphaessemyhy@gmail.com

1. INTRODUCTION

The high reliability of induction machines (IM) is the main advantage which allows these machines to occupy an important place in industrial applications. A more reliable modeling of the physical phenomena governing the operation of IM, allows the development and implementation of linear [1] and non-linear [2]−[6] control strategies, allowing IM to have performances comparable or superior to those of DC machine [7]. Well known simplifying assumptions (isotropy of the machine, parameters invariance, neglected saturation [8]) lead to state models with constant parameters [9]. However, the stator and rotor inductances and resistances are variable due to saturation [10]−[13], and temperature rise [14]−[18]. Design of linear control laws based on these assumptions, are limited and are valid for a given fixed operating point. Nonlinear control strategies are developed based on the linear model without saturation [2], [17], [18], or on the model with saturation [3], [11], [19], [20], which allow to follow the speed and the flux references with accuracy depending on the complexity and the knowledge of the IM parameters.

In this paper, starting from a nonlinear model of the rotor flux [16], we develop a nonlinear control law based on the backstepping technique (NLB), taking into acount the fact that the inductances (stator, rotor and magnetizing) of the IM machine depend on the magnetizing current. We use the rotor flux orientation (FOC)-which is the most used in literature-to deduce the control voltages. Robustness of this control law, with respect to heating, will be investigated and discussed in this article. For the symbols used, the reader can refer to Table 1.

Table 1. List of symbols

Symbol	Designation
u_{sx}, u_{sy}	Stator voltages in the rotor flux-oriented reference frame
i_{sx}, i_{sy}	Stator currents in the rotor flux-oriented reference frame
i_{mr}	Rotor magnetizing current (A) in the rotor flux-oriented reference frame
$|\Psi_r| = L_m|i_{mr}|$	Rotor flux magnitude (Wb)
$|\Psi_r|_{ref}$	Rotor flux reference (Wb)
$L_s(L_r)$	stator (rotor) inductance (H)
L_m	Magnetizing inductance (H)
$R_s(R_r)$	Stator (rotor) resistance (Ω)
$L_{r\sigma} = L_m - L_r$	Rotor leakage inductance (H)
T_r, T_r^*	Rotor time-constant, modified rotor time-constant
ω_r	Electrical speed (rad/s)
ω_g	General reference frame
ω_{rref}	Speed reference (rad/s)
T_{em}, T_L	Electromagnetic torque (Nm), Load torque (Nm)
$\sigma = 1 - \dfrac{L_m^2}{L_s L_r}$	Total leakage factor
E	DC bus voltage (V)
NLB	Nonlinear backstepping controller
FO	Flux observer
$IMNS$	Induction motor with saturated
$IMNS$	Induction motor not saturated

2. MATHEMATICAL MODEL OF IM TAKING INTO ACCOUNT SATURATION

In the literature, several articles have studied the magnetic saturation in induction machines (IM) [3], [21]−[26]. The control laws based on the saturation of the IM machine are: linear controls with update of one or more parameters, or a nonlinear control with constant or variable parameters [27]. The dynamic model of the IM that takes into account saturation of the iron core in [24] will be used to develop a nonlinear control law for speed and flux. Starting from [24], the mathematical model of IM, which takes into account the saturation effect is described by the following state as in (1).

$$\frac{di_{sx}}{dt} = -c_1 i_{sx} + \left(\omega_g + c_2 T_r(\omega_g - \omega_r)\right)i_{sy} + c_3 i_{mrx} - \left((c_3 T_r - a_{21}^* f_1 T_r^*)\omega_g - c_3 T_r \omega_r\right)i_{mry} - c_2 \frac{i_{sx}^2}{i_{mrx}} + f_1 u_{sx}$$

$$\frac{di_{sy}}{dt} = -c_1 i_{sy} - \left(\omega_g + c_2 T_r(\omega_g - \omega_r)\right)i_{sx} + c_3 i_{mry} + \left((c_3 T_r - a_{21}^* f_1 T_r^*)\omega_g - c_3 T_r \omega_r\right)i_{mrx} - c_2 \frac{i_{sy}^2}{i_s} . + f_1 u_{sy}$$

$$\frac{di_{mrx}}{dt} = a_{22}^* i_{sx} - a_{22}^* i_{mrx} + a_{22}^* T_r(\omega_g - \omega_r)i_{mry}$$

$$\frac{di_{mry}}{dt} = a_{22}^* i_{sy} - a_{22}^* i_{mry} - a_{22}^* T_r(\omega_g - \omega_r)i_{mrx}$$

$$\frac{d\omega_r}{dt} = -a_{33}\omega_r + f_3(i_{mrx}i_{sy} - i_{mry}i_{sx}) - f_4 T_L \tag{1}$$

In the rotor frame reference, which rotates at speed $\omega_g = \omega_{mr} = \omega r + a22\frac{i_{sy}}{i_{mrx}}$, the model (1) becomes :

$$\frac{di_{sx}}{dt} = -c_1 i_{sx} + \omega_r i_{sy} + (a_{22} + c_2)\frac{i_{sy}^2}{i_{mrx}} + c_3 i_{mrx} - c_2 \frac{i_{sx}^2}{i_{mrx}} + f_1 u_{sx}$$

$$\frac{di_{sy}}{dt} = -(a_{11} - c_2)i_{sy} - \omega_r i_{sx} - (a_{22} + c_2)\frac{i_{sx}i_{sy}}{i_{mrx}}i_{sd} + c_3 i_{mrq} + \frac{f_1 a_{21}}{a_{22}}\omega_r i_{mrx} - c_2 \frac{i_{sy}^2}{i_{mrx}} + f_1 u_{sy}$$

$$\frac{di_{mrx}}{dt} = a_{22}^*(i_{sx} - i_{mrx})$$

$$\frac{d\omega_r}{dt} = -a_{33}\omega_r + f_3 i_{mrx} i_{sy} - f_4 T_L \tag{2}$$

So, the electromagnetic torque is given by the (3).

$$T_{em} = f_2 i_{mrx} i_{sy} \tag{3}$$

Coefficients that appear in (1)-(3) are defined by the (4).

$$a_{11}^* = \frac{R_s}{\sigma L_s} + \frac{1-\sigma}{\sigma T_r^*}, a_{12}^* = \frac{1}{\sigma L_s T_r^*}, a_{21}^* = L_s\frac{1-\sigma}{T_r^*}, a_{22}^* = \frac{1}{T_r^*}, a_{33} = \frac{b_r}{J_m}, f_1 = \frac{1}{\sigma L_s}, f_2 = \frac{3}{2}p\frac{L_m^2}{L_r}, f_3 = \frac{p}{J_m}f_2 c_1 = a_{11}^* + a_{12}^*(\Delta L -$$

$$2\Delta L^*), c_2 = a_{12}^* \Delta L^*, c_3 = a_{21}^* f_1 + a_{12}^*(\Delta L - \Delta L^*), \Delta L = L - L_m, \Delta L^* = \frac{L_{\sigma r}^2}{L_r^2}\Delta L \tag{4}$$

T_r^* and L are called modified rotor time-constant and dynamic magnetizing inductance, respectively, and are defined as in (5) and (6).

$$T_r^* = T_r \frac{L}{L_m}, \tag{5}$$

$$L = \frac{d|\Psi_r|}{d|i_{mr}|} = L_m + |i_{mr}| \frac{dL_m}{d|i_{mr}|} \tag{6}$$

These equations can be rewritten in a more condensed form as (7) and (8).

$$\frac{di_{sx}}{dt} = F_x + f_1 u_{sx} \tag{7}$$

$$\frac{di_{sy}}{dt} = F_y + f_1 u_{sy} \tag{8}$$

With:

$$F_x = -c_1 i_{sx} + \omega_r i_{sy} + (a_{22} + c_2) \frac{i_{sy}^2}{i_{mrx}} + c_3 i_{mrx} - c_2 \frac{i_{sx}^2}{i_{mrx}}, F_y = -(a_{11} - c_2)i_{sy} - \omega_r i_{sx} - $$

$$(a_{22} + c_2) \frac{i_{sx} i_{sy}}{i_{mrx}} i_{sd} + c_3 i_{mry} + \frac{f_1 a_{21}}{a_{22}} \omega_r i_{mrx} - c_2 \frac{i_{sy}^2}{i_{mrx}}. \tag{9}$$

2.1. Modeling of the rotor flux of IM

In general, saturation curve is a hysteresis form. In our model, only the first magnetization curve is considered. Based on the procedure described in [8], the magnetization curve of the IM is shown in Figure 1. A mathematical model is described by the (10) [24].

$$|\Psi_r| = \alpha\left(1 - e^{-\beta|i_{mr}|}\right) + \gamma|i_{mr}| \tag{10}$$

From (10), an analytical expression of L_m is obtained by (11).

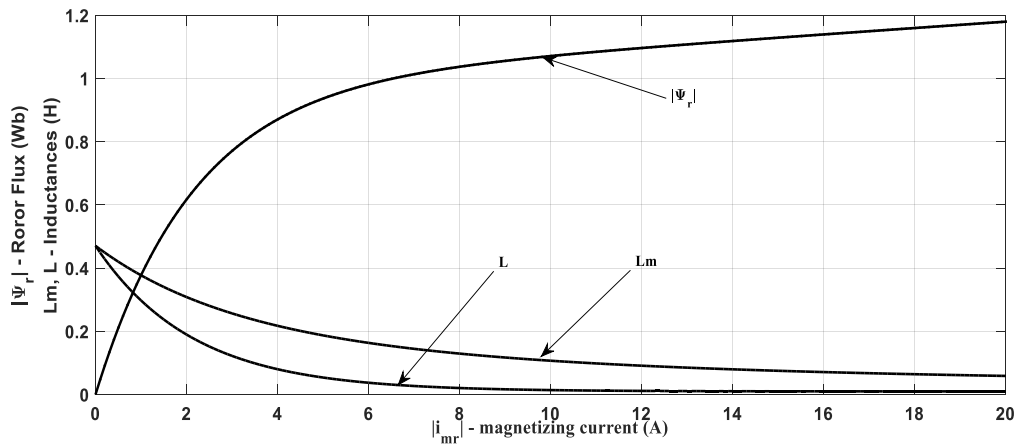$$L_m = \frac{|\Psi_r|}{|i_{mr}|} = \frac{\alpha\left(1 - e^{-\beta|i_{mr}|}\right)}{|i_{mr}|} + \gamma \tag{11}$$

Figure 1. Typical rotor flux curve $|\Psi r|$, magnetizing inductance (L_m) and modified inductance (L)

Notes:
1) Some advantages over polynomial interpolation should be noted:
− This model has three parameters to be identified/optimized
− The three parameters are physically interpretable (have a physical meaning)

- It can be used to analyse and predict the behaviour of the machine for magnetizing currents that exceed the nominal value

2) Inductances can be deduced by a simple derivation. An interesting physical interpretation of the coefficients α, β and γ can be made. Indeed:

- $\lim\limits_{|i_{mr}|\to 0} L_m = \alpha\beta + \gamma$: This means that the tangent of the magnetization curve at the origin is equal to $\alpha\beta+\gamma$. This value represents the initial magnetic state of the iron core.

- $\lim\limits_{|i_{mr}|\to +\infty} L_m = \gamma$: Thus γ represents an inductance. It can be interpreted as magnetizing inductance when the machine is completely saturated.

2.2. Flux observer (FO)

The flux is usually difficult or inaccessible to measure. Therefore, it is necessary to construct a flux observer (FO) that makes the rotor flux available for the synthesis of the proposed nonlinear backstepping (NLB) technique. Let's consider the two state equations of the magnetizing current of (1), and replace i_{mrx} and i_{mry} currents by their estimates $\hat{\imath}_{mrx}$ et $\hat{\imath}_{mry}$. Thus, we rewrite the two components of the magnetizing current as (12):

$$
\begin{aligned}
\frac{d\hat{\imath}_{mrx}}{dt} &= a_{22}^*\left(i_{sx} - \hat{\imath}_{mrx} + T_r(\omega_g - \omega_r)\hat{\imath}_{mry}\right) \\
\frac{d\hat{\imath}_{mry}}{dt} &= a_{22}^*\left(i_{sy} - \hat{\imath}_{mry} - T_r(\omega_g - \omega_r)\hat{\imath}_{mrx}\right)
\end{aligned}
\tag{12}
$$

The resulting errors are ($\tilde{\imath}_{mrx} = i_{mrx} - \hat{\imath}_{mrx}$ et $\tilde{\imath}_{mry} = i_{mry} - \hat{\imath}_{mry}$), and as in (13):

$$
\begin{aligned}
\frac{d\tilde{\imath}_{mrx}}{dt} &= -a_{22}^*\left(\tilde{\imath}_{mrx} - T_r(\omega_g - \omega_r)\tilde{\imath}_{mry}\right) \\
\frac{d\tilde{\imath}_{mry}}{dt} &= -a_{22}^*\left(\tilde{\imath}_{mry} + T_r(\omega_g - \omega_r)\tilde{\imath}_{mry}\right)
\end{aligned}
\tag{13}
$$

Consider the following Lyapunov candidate function as in (14).

$$
V_{obs} = \frac{1}{2}\left(\tilde{\imath}^2{}_{mrx} + \tilde{\imath}^2{}_{mry}\right)
\tag{14}
$$

Its dynamics is given by (15).

$$
\dot{V}_{obs} = \tilde{\imath}_{mrx}.\dot{\tilde{\imath}}_{mrx} + \tilde{\imath}_{mry}.\dot{\tilde{\imath}}_{mry} = -a_{22}^*\left(\tilde{\imath}^2{}_{mrx} + \tilde{\imath}^2{}_{mry}\right)
\tag{15}
$$

Since $a_{22}^* > 0$ then the FO is globally asymptotically stable.

In the rotor flux-oriented reference frame, the magnetizing current ($|i_{mr}| = i_{mrx}$) rotates at the speed ω_{mr}, which allows to write as in (16) and (17).

$$
\frac{d\hat{\imath}_{mrx}}{dt} = a_{22}^*(i_{sx} - \hat{\imath}_{mrx})
\tag{16}
$$

$$
\omega_{mr} = \omega_r + a_{22}\frac{i_{sy}}{i_{mrx}}
\tag{17}
$$

Then the rotor flux will be deduced from (10), (11) and (16), (17). Figure 2 shows the block diagram of the flux observer (FO):
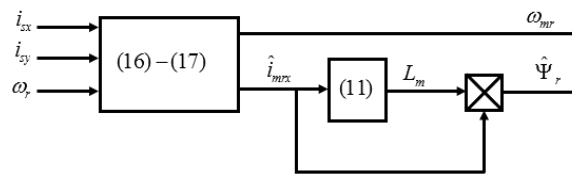

Figure 2. Block diagram of the flux observer (FO)

3. DESIGN AND ANALYSIS OF SPEED AND FLUX BACKSTEPPING CONTROLLER (NLB)

We are interested in rotor speed and rotor flux magnitude control of the IM described by (2). Actual speed of the IM must follow its reference speed whatever the operating mode of the IM is. Synthesis of this nonlinear control law is based on the backstepping technique.

1st step: We define the following tracking error as in (18).

$$e_1 = \omega_r - \omega_{rref} \tag{18}$$

Deriving e_1 with respect to time, we obtain as in (19).

$$\dot{e}_1 = \dot{\omega}_r - \dot{\omega}_{rref} = -a_{33}\omega_r + f_3 i_{mrx} i_{sy} - f_4 T_L - \dot{\omega}_{rref} \tag{19}$$

The term $f_3 i_{mrx} i_{sy}$ is the electromagnetic torque of IM, so the choice of this term as a virtual control appears natural. Thus, we define a new error:

$$z_1 = f_3 i_{mrx} i_{sy} - v_1 \tag{20}$$

The dynamics of z_1, is obtained by deriving (20) with respect to time.

$$
\begin{aligned}
\dot{z}_1 &= \frac{d}{dt}\left(f_2 i_{mrx} i_{sy}\right) - \dot{v}_1 = \frac{3}{2}\frac{p^2}{J_m}\left[\frac{d\left(\frac{L_m^2}{L_r}\right)}{dt}\cdot i_{mrx} i_{sy} + \frac{L_m^2}{L_r}\cdot\frac{d}{dt}\left(i_{mrx} i_{sy}\right)\right] - \dot{v}_1 \\
&= f_3\left[a_{22}^*\left(\left(\frac{2}{L_m} - \frac{1}{L_r}\right)\Delta L + 1\right)\left(i_{sx} - i_{mrx}\right)i_{sy} + i_{mrx}\cdot f_y(x)\right] + f_3 f_1 i_{mrx} u_{sy} - \dot{v}_1
\end{aligned}
\tag{21}
$$

The magnetizing current of the rotor i_{mrx} is not measurable because it is difficult to access, we replace it, in the control law, by its estimate $\hat{i}_{mrx}$ and we rewrite $\dot{z}_1$ in a condensed form (22).

$$\dot{z}_1 = \mu_1 + a_1 u_{sy} \tag{22}$$

With:

$$\mu_1 = f_3\left[\left(\left(\frac{2}{L_m} - \frac{1}{L_r}\right)\Delta L + 1\right)\frac{d\hat{i}_{mrx}}{dt}\cdot i_{sy} + \hat{i}_{mrx}\cdot f_y(x)\right] - \dot{v}_1; a_1 = f_3 f_1 \hat{i}_{mrx}$$

Notes:

The dynamics of the magnetizing and rotor inductances ($\frac{dL_m}{dt}$ and $\frac{dL_r}{dt}$) are given by (23).

$$
\begin{cases}
\frac{dL_m}{dt} = \frac{dL_m}{di_{mrx}}\cdot\frac{di_{mrx}}{dt} = \frac{L - L_m}{i_{mrx}}\cdot\frac{di_{mrx}}{dt} = \frac{\Delta L}{i_{mrx}}\cdot\frac{di_{mrx}}{dt} \\
\frac{dL_r}{dt} = \frac{d(L_{\sigma r} + L_m)}{dt} = \frac{dL_m}{dt}
\end{cases}
\tag{23}
$$

Rotor inductance is no longer constant, it depends on the magnetizing inductance, thus on the magnetizing i_{mrx} current. Leakage $L_{\sigma r}$ inductance is assumed to be constant, this assumption is common to that of [16] and [3]. But the rotor inductance depends on the magnetizing inductance: $L_r = L_{\sigma r} + L_m$, which makes it depends on the magnetizing inductance. Consider the following Lyapunov candidate function as in (24).

$$V_1 = \frac{1}{2}(e_1^2 + z_1^2) \tag{24}$$

The dynamics of is V_1 given by (25).

$$\dot{V}_1 = e_1\dot{e}_1 + z_1\dot{z}_1 = e_1\left(-a_{33}\omega_r + v_1 - f_4 t_L - \dot{\omega}_{rref}\right) + z_1\left(e_1 + \mu_1 + a_1 u_{sy}\right) \tag{25}$$

To have global asymptotic stability, must $\dot{V}_1$ verify the following condition by (26).

$$\dot{V}_1 = -k_1 e_1^2 - d_1 z_1^2 \tag{26}$$

Where k_1 and d_1 are any positive real design constants. By identifying (25) to (26), we obtain the (27).

$$\begin{cases} -k_1 e_1 = -a_{33}\omega_r + v_1 - f_4 t_L - \dot{\omega}_{rref} \\ -d_1 z_1 = e_1 + \mu_1 + a_1 u_{sy} \end{cases} \tag{27}$$

2^{nd}step: the nonlinear controller must follow the flux reference. We denote $\widehat{\Psi}_r$ the estimate of rotor flux Ψ_r. So, we define the following error as (28).

$$e_2 = \left|\widehat{\Psi}_r\right|^2 - |\Psi_r|^2_{ref} \tag{28}$$

Then we derive e_2 with respect to time, we obtain (29).

$$\begin{aligned} \dot{e}_2 &= 2\left|\hat{\Psi}_r\right|\left|\dot{\Psi}_r\right| - 2|\Psi_r|_{ref}\left|\dot{\Psi}_r\right|_{ref} = 2\left|\hat{\Psi}_r\right|L\frac{di_{mrx}}{dt} - 2|\Psi_r|_{ref}\left|\dot{\Psi}_r\right|_{ref} \\ &= 2a_{22}L_m^2\hat{i}_{mrx}i_{sx} - 2a_{22}\left|\hat{\Psi}_r\right|^2 - 2|\Psi_r|_{ref}\left|\dot{\Psi}_r\right|_{ref} \end{aligned} \tag{29}$$

We choose the term as $2a_{22}L_m^2\hat{i}_{mrx}i_{sx}$ a second virtual command and define a new error z_2 as (30).

$$z_2 = 2a_{22}L_m^2\hat{i}_{mrx}i_{sx} - v_2 \tag{30}$$

The dynamics of z_2 is given by (31).

$$\begin{aligned} \dot{z}_2 &= 4a_{22}L_m\frac{dL_m}{dt}\hat{i}_{mrx}i_{sx} + 2a_{22}L_m^2 i_{sx}\frac{d\hat{i}_{mrx}}{dt} + 2a_{22}L_m^2\hat{i}_{mrx}\frac{di_{sx}}{dt} - \dot{v}_2 \\ &= 2a_{22}L_m\left[a_{22}^*(2\Delta L + L_m)i_{sx}(i_{sx} - i_{mrx}) + \left|\hat{\Psi}_r\right|f_x(x)\right] + 2a_{22}L_m\left|\hat{\Psi}_r\right|u_{sx} - \dot{v}_2 \end{aligned} \tag{31}$$

We rewrite (31) in a more condensed form (32).

$$\dot{z}_2 = \mu_2 + a_2 u_{sx} \tag{32}$$

With: $\mu_2 = 2a_{22}L_m\left[a_{22}^*(2\Delta L + L_m)i_{sx}(i_{sx} - i_{mrx}) + \left|\widehat{\Psi}_r\right|f_x(x)\right] - \dot{v}_2; a_2 = 2a_{22}L_m\left|\widehat{\Psi}_r\right|$.

We consider the new Lyapunov candidate function defined by (33).

$$V_2 = \frac{1}{2}(e_2^2 + z_2^2) \tag{33}$$

Its derivative with respect to time is given by (34).

$$\dot{V}_2 = e_2\dot{e}_2 + z_2\dot{z}_2 = e_2\left(v_2 - 2a_{22}\left|\widehat{\Psi}_r\right|^2 - 2|\Psi_r|_{ref}\left|\dot{\Psi}_r\right|_{ref}\right) + z_2(e_2 + \mu_2 + a_2 u_{sx}) \tag{34}$$

To have global asymptotic stability, $\dot{V}_2$ must satisfy by (35)

$$\dot{V}_2 = -k_2 e_2^2 - d_2 z_2^2 \tag{35}$$

Where k_2 and d_2 are any positive real design constants.

By identifying (34) to (35), we obtain the (36).

$$\begin{cases} -k_2 e_2 = v_2 - 2a_{22}\left|\widehat{\Psi}_r\right|^2 - 2|\Psi_r|_{ref}\left|\dot{\Psi}_r\right|_{ref} \\ -d_2 z_2 = e_2 + \mu_2 + a_2 u_{sx} \end{cases} \tag{36}$$

According to (27) and (36) the control voltages u_{sx} and u_{sy} satisfy as in (36) and (37).

$$u_{sy} = \frac{-e_1 - d_1 z_1 - \mu_1}{a_1} \tag{37}$$

$$u_{sx} = \frac{-e_2 - d_2 z_2 - \mu_2}{a_2} \tag{38}$$

Now we need to calculate the derivatives of the virtual commands $\dot{v}_1$ and $\dot{v}_2$. Using (27) and (36) we obtain:

$$\begin{cases} \dot{v}_1 = -k_1 \dot{e}_1 + a_{33} \dot{\omega}_r + f_4 \dot{t}_L + \ddot{\omega}_{rref} \\ \quad = -a_{33}(a_{33} - k_1)\omega_r + f_3(a_{33} - k_1)\hat{\imath}_{mrx} i_{sy} - f_4((a_{33} - k_1)t_L + 1)\dot{t}_L + k_1 \dot{\omega}_{rref} + \ddot{\omega}_{rref} \\ \dot{v}_2 = -k_2 \dot{e}_2 + 4a_{22}|\widehat{\Psi}_r| \left|\dot{\widehat{\Psi}}_r\right| + 2|\Psi_r|_{ref}^2 + 2|\Psi_r|_{ref}|\ddot{\Psi}_r|_{ref} \\ \quad = 2(2a_{22} - k_2)|\Psi_r||\dot{\Psi}_r| + 2|\Psi_r|_{ref}^2 + 2\left(k_2|\dot{\Psi}_r|_{ref} + |\ddot{\Psi}_r|_{ref}\right)|\Psi_r|_{ref} \end{cases}$$

4. SIMULATION RESULTS AND DISCUSSION

The controller gains are selected as $d_1 = 1.10^3, k_1 = 7.10^4, k_2 = 7.10^4, d_2 = 0.1.10^3$. The choice of the controller gain and the adaptive gain is not arbitrary. So, if this choice is correct, we get a high performance of the NLB controller. In a first test, rotor flux and speed references are set to 1 Wb and 100 rad/s respectively. At 1 second, nominal load torque of 15 Nm is applied to IM. Figures 3(a)-(e) shows simulation results of this first test.

It can be seen that rotor speed reaches its reference of 100 rad/s (Figure 3(a), in about *16ms* with an absolute error of less than 0.08 rad/s in Figures 3(b)-(c)), before and after the application of the load torque. At the moment of application of 15 Nm load torque, the absolute error of speed does not exceed 1.8rad/s, before it returns to the range of 0.08 rad/s. Rotor flux -necessary for the synthesis of the control law- is estimated using the nonlinear flux observer (FO) depicted in Figure 2. Induction machine (IM) produces a rotor flux that follows well its reference (Figure 3(d). Before applying load torque, the absolute flux error is about 9 mWb, while after applying this torque, this error decreases to 3 mWb, but in all cases this error does not exceed 10 mWb (Figure 3(d)).

Electromagnetic torque developed by the machine compensates the load torque Figure 4(a). In this test it is assumed that the friction is part of the load torque, and it is assumed to be known or estimated, and its first derivative exists. Figure 4(b) shows the error between the electromagnetic torque and the load torque. This error is zoomed in to see the effect of applying the load Figure 4(c), it shows that this error does not exceed 1.5 Nm before and after the load torque was applied. A torque peak is observed at time 1 second which is quickly cancelled by the control. i_{sx} current component evolves in the same way as the rotor flux, and i_{sy} current component evolves in the same way as the electromagnetic torque. This result is common to the classical FOC, and it is also confirmed by in (3) and (10) as shown in Figures 3(d)-(e).

Stator currents have a profile that confirms the torque and flux in (3) and (16). Indeed, in steady state, i_{sx} current component controls the rotor flux (in (2) and (10)) and Figure 4(d) shows this dependence. i_{sy} current component is responsible produces the electromagnetic torque (in (3)), because in steady state ($i_{mrx} = i_{sx}$) and therefore the electromagnetic torque depends essentially on i_{sy} as shown in Figure 4(e).

As long as inductances L_m and L are constant, currents i_{sx} and i_{sy} are also constant. Variation of rotor time-constant T_r is also due to the variation of IM inductances ($L_r, L_s, L_m, \dots$). Figure 5(a) shows the variation of the rotor time-constant, the magnetizing and modified inductances obtained by the first test. Initially, both inductances L_m and L start from, $L_m = L = 0.4695\,H$, which explains the peaks of current and electromagnetic torque observed at the beginning of the simulation, then they decrease until they stabilize, at no load ($T_L = 0$), to the values : $L_m = 0.1477\,H$ and $L = 0.028\,H$ respectively. After applying load torque, the values of inductances increase slightly and become respectively: $L_m = 0.1514\,H$ and $L = 0.030\,H$. Figure 5(b) gives the two time-constants introduced in the IMWS model. Initially the two time-constants described in the IMWS model, have the following values: $T_r = T_r^* = 0.3107\,s$, then they decrease to $T_r = 0.103\,s$ and $T_r^* = 0.0199\,s$. After applying load torque, these values slightly increase to $T_r = 0.105\,s$ and $T_r^* = 0.0212\,s$. From these results, it can be concluded that the model that takes into account the magnetic saturation, is valid to describe the variable behavior of inductances and the rotor time-constant *(at constant rotor resistance)*. Figures 3 to 5 show, that rotor speed and flux are well controlled by the proposed nonlinear control law (NLB), despite the variation of several parameters such as the rotor (L_r), stator (L_s) and magnetizing (L_m) inductances and the rotor time-constant (T_r).

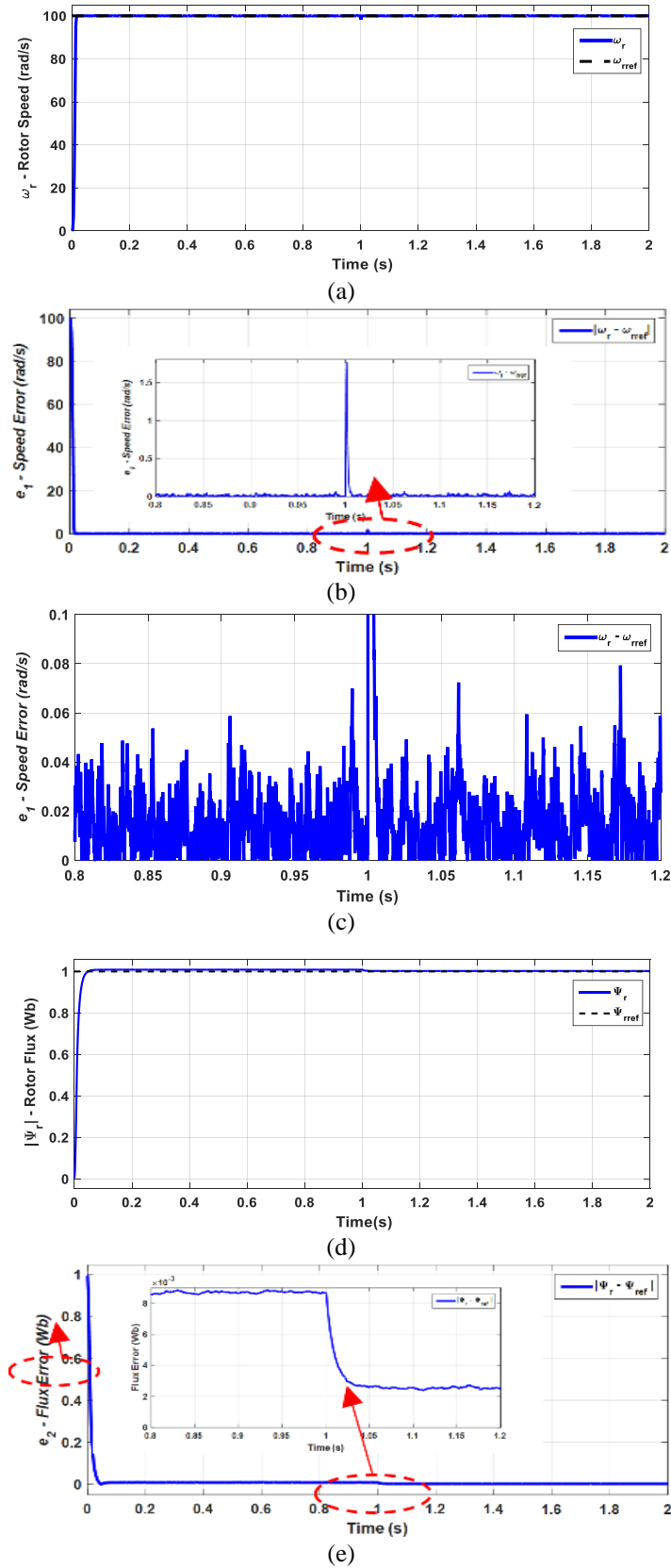Figure 3. Simulation results for references $|\psi_r|_{ref}$ =1 Wb and $\omega_{r,ref}$ =100 rad/s; (a) rotor speed, (b) absolute speed error $\left(\left|\omega_r - \omega_{rref}\right|\right)$, (c) zoom around the moment of application of the load torque (between 0.8 and 1.2 seconds), (d) 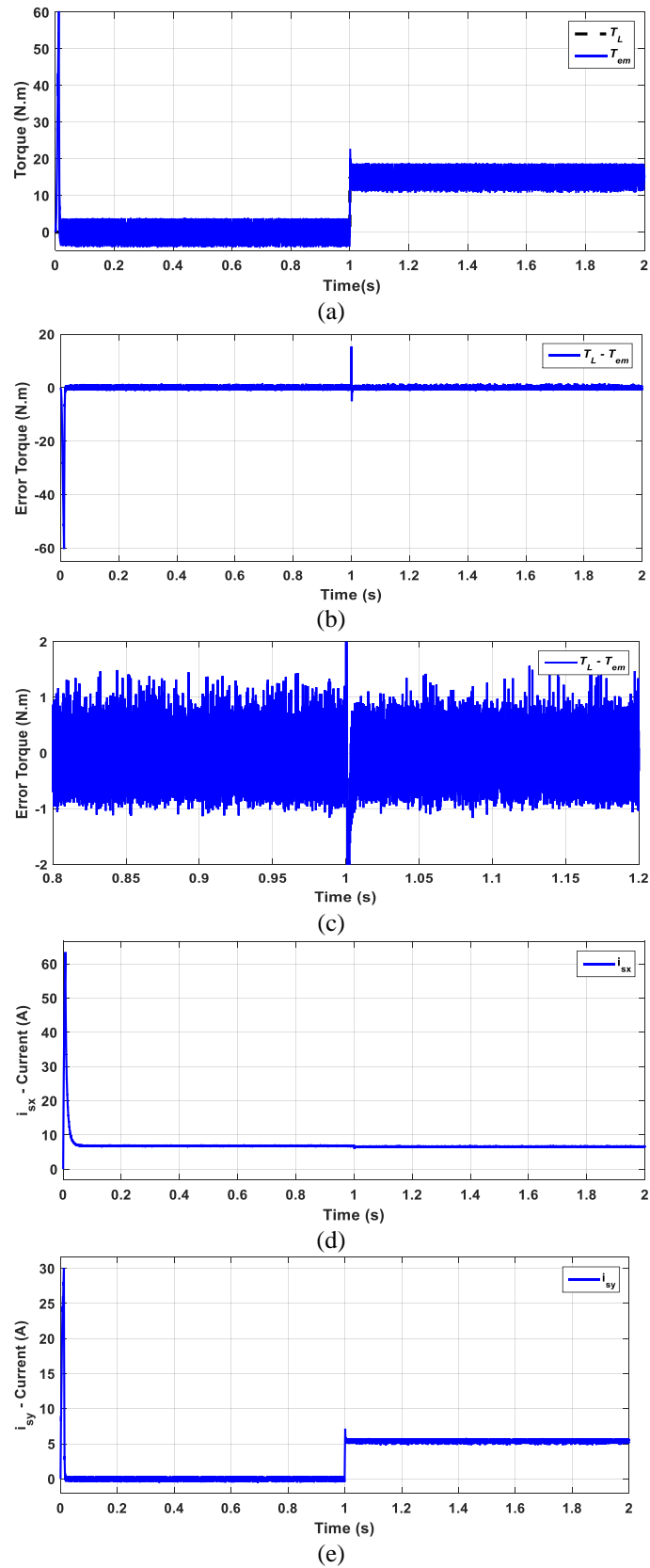measured rotor flux of IM, and (e) absolute flux error $\left(\left|\left|\Psi_r\right| - \left|\Psi_r\right|_{ref}\right|\right)$

Figure 4. Simulation results for references $|\psi_r|_{ref}$=1 Wb and $\omega_{r,ref}$ =100 rad/s; (a) electromagnetic torque at no load and when applying a 15 N.m load torque, (b) the torque error $(T_L - T_{em})$, (c) zoomed view of the torque error $(T_L - T_{em})$, (d) and (e) stator currents i_{sx} and i_{sy} respectively

4.1. Influence of the rotor resistance variation

In a second test, the speed of the machine is fixed at 100 rad/s and the rotor flux at 1 Wb. The objective of this second test is:

− to compare the proposed control law in the case where the model of the induction machine takes into account saturation and in the case where the inductances are assumed constant;
− to test the robustness of this control strategy (NLB) with respect to the heating of IM (increase of rotor resistanceR_r). Simulation results are shown in the Figure 6.

Figure 6 shows the speed of the induction machine for different values of the rotor resistance, considering constant rotor speed and flux. It can be seen that the increase of the rotor resistance (by heating) has no influence on the steady state speed, neither in the IMWS case Figure 6(a) nor in the IMNS case Figure 6(c). However, the influence of the rotor resistance is clearly seen in transient state. The increase of the rotor resistance allows the speed to reach its reference faster as shown in Figures 6(b)-(d). Indeed, if $R_r = 0.5R_{rn}$ the motor speed reaches their reference at 0.02 seconds, and if $R_r = 2R_{rn}$, the speed reaches its reference after 0.01 seconds. This is justified by the fact that the rotor time constantT_r decreases with increasing resistance, so the speed response becomes faster.

Figure 7 shows the rotor flux produced (measured) by IM when taking into account the saturation (IMWS case) Figures 7(a) and 7(b) and when assuming no saturation (IMNS case) Figures 7(c)-(d) following a variation of the rotor resistance. In steady state, we note that by increasing the rotor resistance, the real flux produced by IM stabilizes at its reference of 1 Wb see Figures 7(a) and (c)) However, in transient mode, the rise time of each flux depends on the rotor resistance value.

Indeed, for$R_r = 0.5R_{rn}$, the flux reaches the reference after 0.25 s in the IMWS case Figure 7 (b), and after *1s* in the IMNS case Figure 7(d). Whereas for $R_r = 2R_{rn}$, the flux reaches its reference more quickly, but it presents an overshoot. This overshoot increases with increasing rotor resistor value. In transient state, the difference between IMWS and IMNS cases is clear. In the IMWS case, the maximum overshoot is about 20 %, but in the IMNS case, this overshoot reaches 70 %. This is due to the fact that the magnetic saturation limits the overshoot to 1.2 Wb (flux of the saturated machine). However, in the IMNS case this limit does not exist because the flux is assumed to be linear (constant inductance). On the other hand, the flux response is faster in the case with saturation (IMWS) than in the case without saturation see Figures 7(b)-(d).
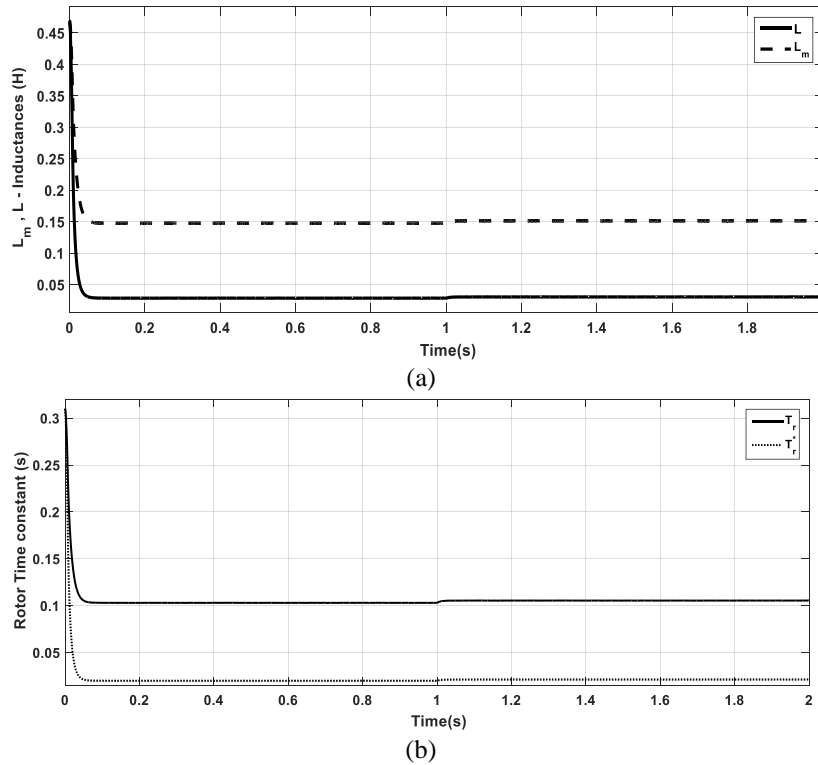

(a)

(b)

Figure 5. Motor's parameters variation during the first test (a) magnetizing and modified inductance and (b) rotor and modified time-constants
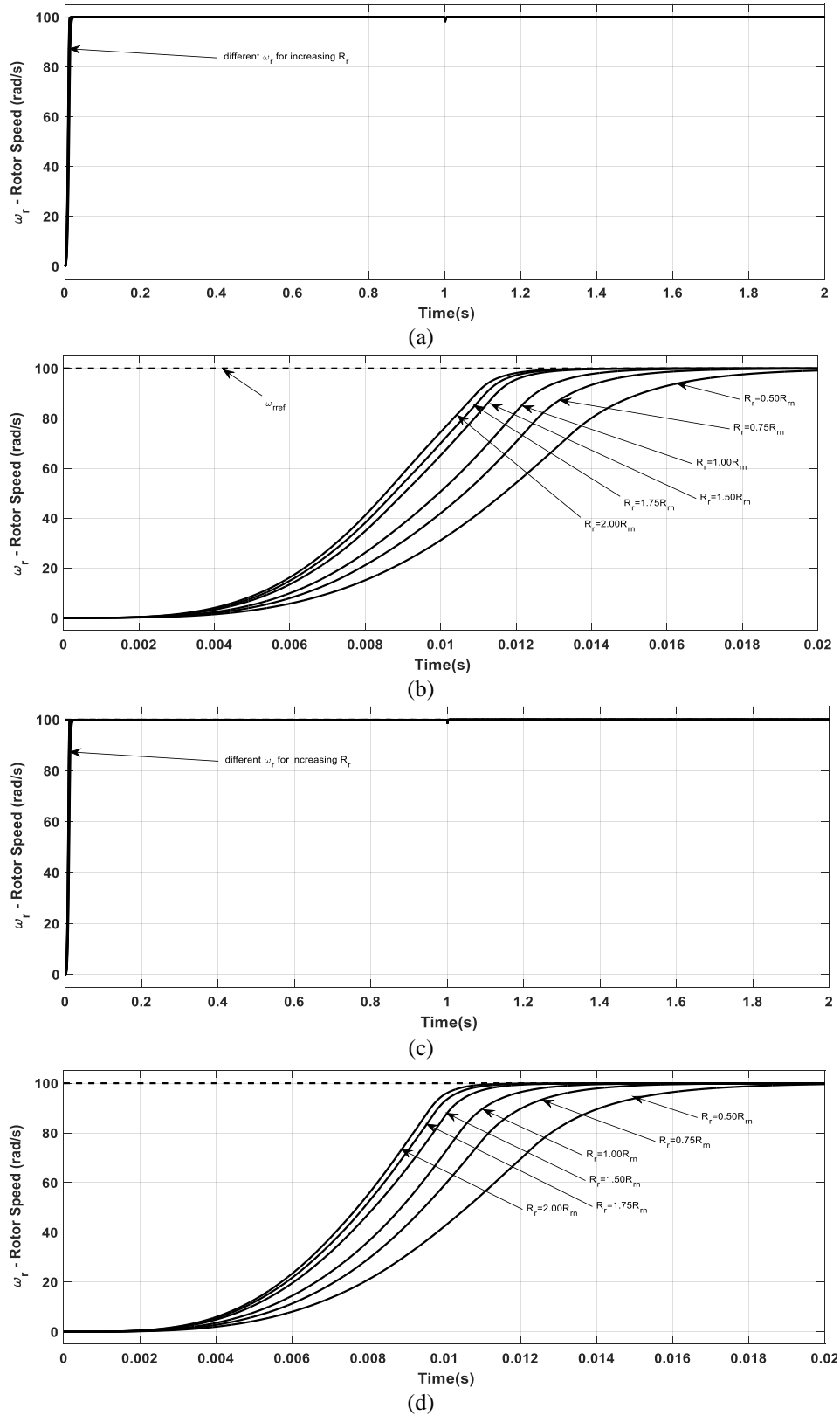
Figure 6. Resulting speed for references $|\psi_r|_{ref}$=1 Wb and $\omega_{r,ref}$ =100 rad/s; (a) IM speed in the IMWS case for increasing of rotor resistanceR_r, (b) zoomed view on time interval [0-0.02 s] in IMWS case, (c) speed in the IMNS case, and (d) zoomed view on time interval [0-0.02 s] in the IMNS case
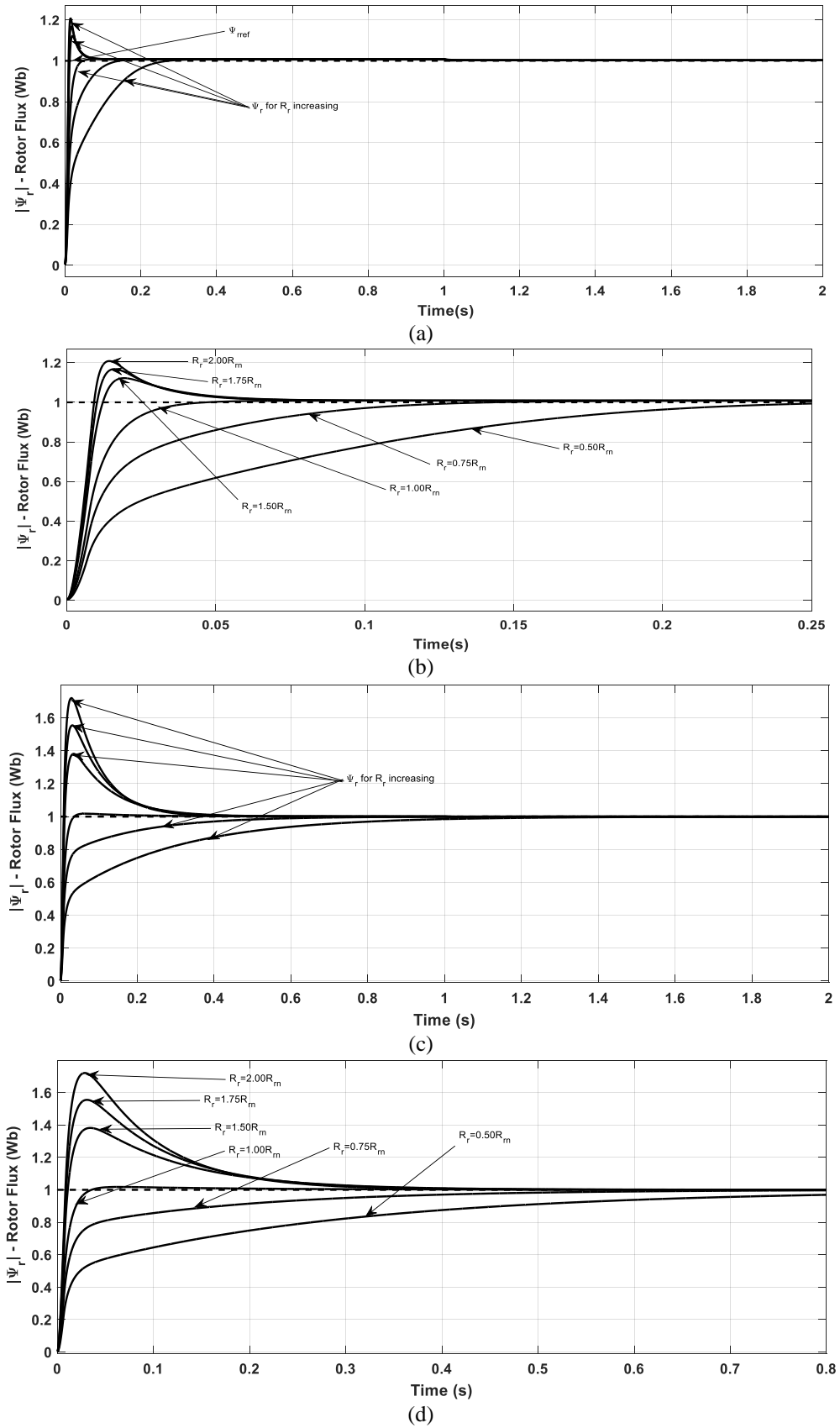
Figure 7. Resulting flux for references $|\psi_r|_{ref}$=1 Wb and $\omega_{r,ref}$ =100 rad/s, (a) actual rotor flux produced by IM in the IMWS case, (b) zoomed view on the transient state (IMWS case), (c) actual rotor flux produced by IM in the IMNS case, and (d) zoomed view on the transient state (IMNS case)

Figure 8(a) shows the electromagnetic torque developed by the machine as a result of variations in the rotor resistance and the modified rotor time-constant used in the IMWS model. In steady state the electromagnetic torque follows the load torque. There is an overshoot at the beginning of operation due to the fact that initially the rotor time-constant is very large compared to its steady state value see Figure 8(b).

(a)

(b)
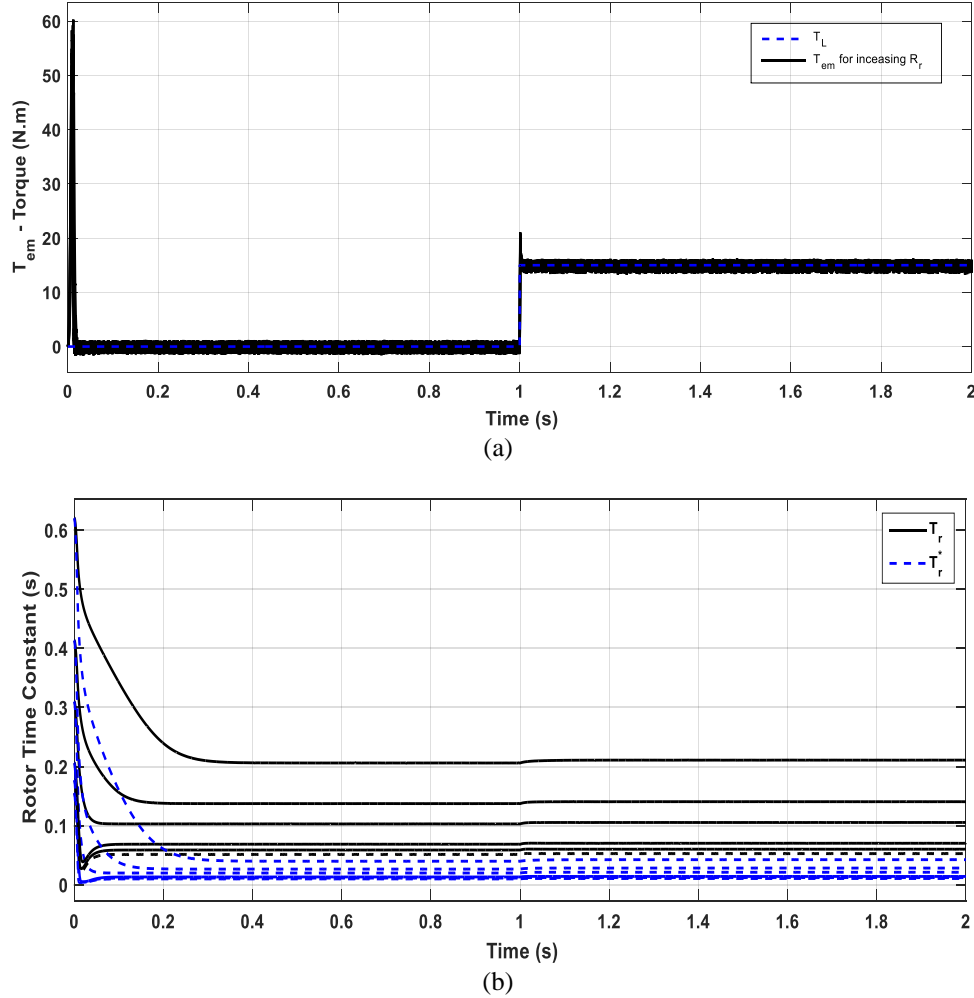
Figure 8. IM electromagnetic torque for references $|\psi_r|_{ref}$=1 Wb and $\omega_{r,ref}$ =100 rad/s, (a) different values of rotor resistance, and (b) rotor and modified time constants in the IMWS case

Table 2 gives a comparison between the IMWS model and IMNS model, using two performances indexes: the first (IAE: Integral of absolute error $IAE = \int_0^\infty |e(t)|dt$), and the second (ITAE: Integral of time multiplied by absolute error $ITAE = \int_0^\infty t|e(t)|dt$). Performance index (IAE, ITAE) is a parameter on the basis of which we can decide the system accuracy and sensitivity. Table 2 shows that the IAE errors of rotor speed, in the IMWS and IMNS cases, are very close and it decrease as the resistance R_r increases. The ITAE error of rotor speed is lower in the IMWS case, compared to the IMNS case. Concerning the flux, we notice that the IAE error is better in the IMWS case than in the IMNS case, and it decreases as the resistance R_r increases. This error remains constant after $R_r = 1.5R_{rn}$. For the ITAE, its values are lower in the case with saturation, than in the case without saturation. Also, it remains constant after $R_r = 1.5R_{rn}$.

These results confirm that the model, which takes into account the magnetic saturation (i.e, IMS) allows to describe with more accuracy the phenomenon of magnetic saturation. The proposed nonlinear control law (NLB) allows minimizing the speed and flux errors in the presence of heating in IM.

Table 2. IAE and TIAE in the case of the IMWS and IMNS model

| | IMWS Model | | | | IMNS model | | | |
| | $\omega_r - \omega_{rref}$ | | $\|\Psi_r\| - \|\Psi_r\|_{ref}$ | | $\omega_r - \omega_{rref}$ | | $\|\Psi_r\| - \|\Psi_r\|_{ref}$ | |
R_r/R_{rn}	IAE	ITAE	IAE	ITAE	IAE	ITAE	IAE	ITAE
0.5	1.174	0.035	0.064	0.011	1.133	0.087	0.149	0.041
0.75	1.059	0.035	0.032	0.009	1.026	0.101	0.054	0.009
1	0.991	0.034	0.021	0.008	0.961	0.095	0.013	0.001
1.5	0.910	0.038	0.020	0.008	0.890	0.084	0.054	0.006
1.75	0.886	0.041	0.020	0.008	0.863	0.084	0.066	0.006
2	0.865	0.042	0.020	0.008	0.847	0.081	0.076	0.007

4.2. Influence of the variation of the speed and rotor flux references

In this section, we vary both the flux and rotor speed references, assuming constant rotor resistance equal to nominal value ($R_r = 1.0R_{rn}$). Figure 9 shows simulation results for variable reference of speed ($20 \rightarrow 40 \rightarrow 60 \rightarrow 100 rad/s$), rotor flux ($0.2 \rightarrow 0.4 \rightarrow 0.6 \rightarrow 1Wb$) and load torque ($2 \rightarrow 4 \rightarrow 6 \rightarrow 15Nm$). Rotor speed and rotor flux produced by IM are well controlled, even if their references change abruptly Figures 9(a) and 9(b). This shows that the proposed control law can control the speed and flux of IM for different operating points. On the contrary, a PID controller cannot control the machine in these different operating points without resizing it. The electromagnetic torque of the machine confirms the previous results (Figures 9(c)). It is noted that at each transition between two operating points, the torque developed has a large value to quickly stabilize to the new operating point. In steady state, since the magnetizing current i_{mrx} and the stator current i_{sx} are equal, this lets us write:

$$T_{em} = f_2 i_{sx} i_{sy} \tag{39}$$

$$|\Psi_r| = L_m . i_{sx} \tag{40}$$

Therefore, i_{sx} current component controls the rotor flux (see Figures 9(d)) and the electromagnetic torque depends on the two stator current components i_{sx} and i_{sy}. Appropriate control of i_{sx} component makes the torque depend only on i_{sy} component (see Figures 9(e)). However, in the synthesis of NLB, we did not take this particular condition into consideration, but on the contrary, the torque as described by (40) depends (in steady state) on the product of the two stator current components and on the parameter $f_2 = f(i_{mrx}, L_m)$.
Remark:

We can synthesize a control law without using the rotor flux orientation condition: $\left(\omega_g = \omega_{mr} = \omega_r + a_{22}\dfrac{i_{sy}}{i_{mrx}}\right)$ and still obtain the same results. So, to optimize the synthesis, we can use this condition of flux orientation from the beginning and avoid any unnecessary calculation.

4.3. Simulation configuration

In all simulations conducted in this paper, the MATLAB/Simulink environment has been configured as follows:
− Solver: ode8 (Dormand-Prince);
_ Fixed point with a sampling period: T_S= 10 μs;
− Switching frequency: f_d= 5 kHz.
Table 3 gives the nominal values of the asynchronous machine used in this paper:

Table 3. Nominal values of IM

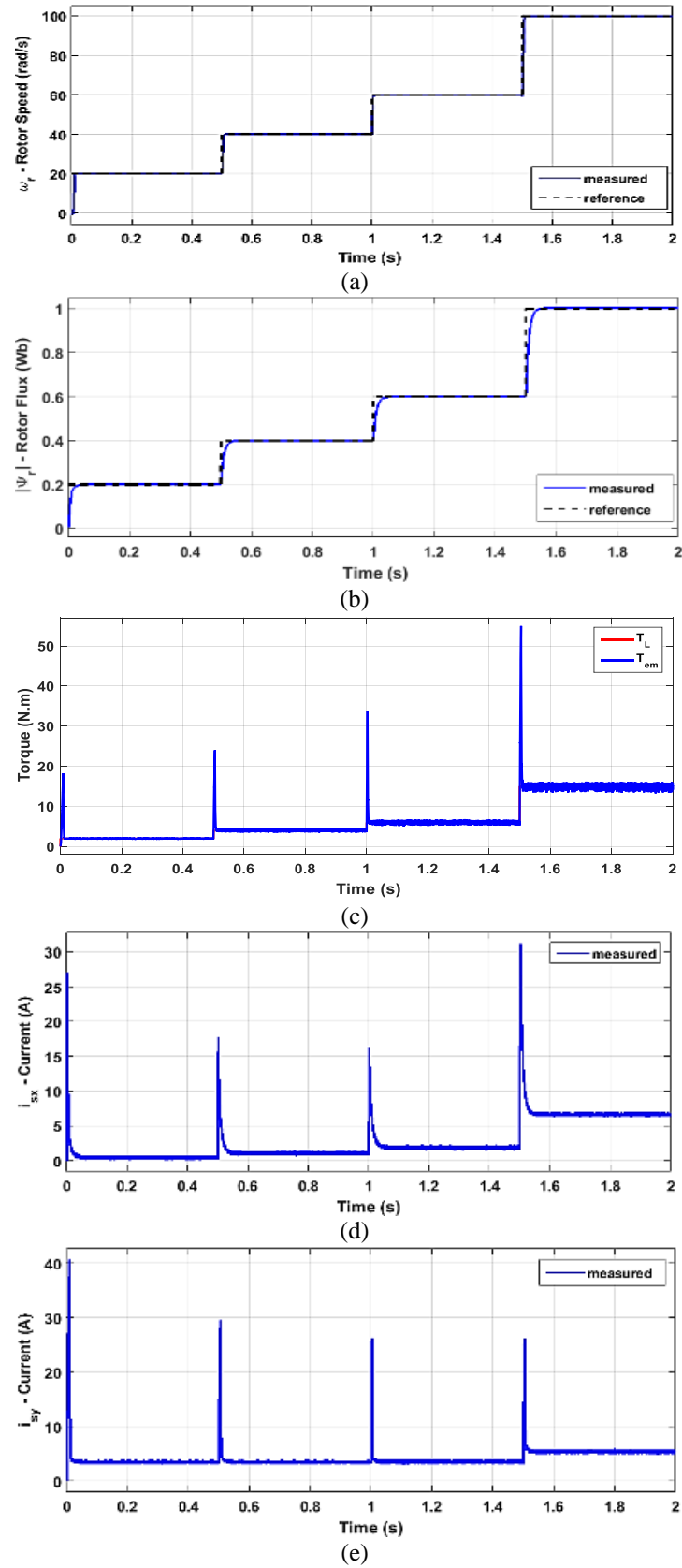| Parameter	Value
Rated Power P_{nom}	2.2 kW
Rated Voltage V_{nom}	220 V
Rated frequency f_{nom}	50 Hz
Rated Torque $T_{em,nom}$	14.9 Nm
Pole pair sp	2
inertia moment J_m	0.0067 kg.m^2
E (DC BUS)	650 V
$L_{\sigma r} = L_{\sigma s}$	0.012 H
R_{sn}	2.90Ω
R_{rn}	1.55 Ω

Figure 9. Simulation results for variable speed and flux references, (a) rotor speed:$20 \rightarrow 40 \rightarrow 60 \rightarrow 100\,rad/s$, (b) rotor flux:$0.2 \rightarrow 0.4 \rightarrow 0.6 \rightarrow 1\,Wb$, (c) load torque, (d) i_{sx} stator current component and (e) i_{sy} stator current component

5. CONCLUSION

In this paper, we have synthesized a nonlinear control law based on the "Backstepping" technique (NLB). Assuming the nonlinear saturated/unsaturated IM models, and consequently variable magnetizing inductance, the NLB accurately performs control of the rotor speed and flux without the need of several control loops. The developed control law gives satisfactory performances in terms of speed, flux and torque, even if the machine parameters change: change of the rotor time-constant, variation of the rotor resistance (heating) and the magnetizing inductance (saturation). In the literature, there is not enough study of the behavior of the control law with respect to the variation of the rotor resistance. Therefore, in this work, we have seen that the proposed control law (NLB) allows to control the speed, the flux and the torque even with the variation of the rotor resistance. The robustness of the control, with respect to IM parameters variation, is extensively tested and compared to the model without saturation.

REFERENCES

[1] D. Telford, M. W. Dunnigan and B. W. Williams, "Online identification of induction machine electrical parameters for vector control loop tuning," *IEEE Transactions on Industrial Electronics*, vol. 50, no. 2, pp. 253-261, 2003, doi: 10.1109/TIE.2003.809397.

[2] M. Madark, A. B. Razzouk, E. Abdelmounim, and M. E. Malah, "A New Induction Motor Adaptive Robust Vector Control based on Backstepping," *International Journal of Electrical and Computer Engineering*, vol. 7, no. 4, pp. 1983-1993, 2017, doi: 10.11591/ijece.v7i4.pp1983-1993.

[3] F. Alonge, M. Cirrincione, M. Pucci and A. Sferlazza, "A Nonlinear Observer for Rotor Flux Estimation of Induction Motor Considering the Estimated Magnetization Characteristic," *IEEE Transactions on Industry Applications*, vol. 53, no. 6, pp. 5952-5965, 2017, doi: 10.1109/TIA.2017.2710940.

[4] F. Alonge, M. Cirrincione, M. Pucci and A. Sferlazza, "Input-output feedback linearization control of linear induction motors including the dynamic end-effects," *IEEE Energy Conversion Congress and Exposition (ECCE)*, 2014, pp. 3562-3569, doi: 10.1109/ECCE.2014.6953885.

[5] M. Comanescu, "Design of estimators for the inverse of the rotor time constant of the induction motor with known flux," *IEEE International Symposium on Sensorless Control for Electrical Drives (SLED)*, 2017, pp. 43-48, doi: 10.1109/SLED.2017.8078428.

[6] B. Mounir, A. Ba-Razzouk, M. Elharoussi, and B. Rached, "Attenuation of voltage sags effects and dynamic performance improvement of a multi-motor system," *International Journal of Power Electronics and Drive Systems*, vol. 13, no. 2, pp. 705-715, 2022, doi: 10.11591/ijpeds.v13.i2.pp705-715.

[7] H. Ouadi, F. Giri, A. Elfadili, and L. Dugard, "Magnetic saturation effect in the achievement of wide speed range control for induction machine," *IFAC Proceedings Volumes*, vol. 42, no. 9, pp. 350-355, 2009, doi: 10.3182/20090705-4-SF-2005.00062.

[8] A. Ba-Razzouk, "Neural network estimation of the rotor time constant of asynchronous machines," PhD Thesis, Montreal, Polytechnic School, 1998.

[9] A. Accetta, F. Alonge, M. Cirrincione, M. Pucci and A. Sferlazza, "Parameter identification of induction motor model by means of state space-vector model output error minimization," *International Conference on Electrical Machines (ICEM)*, 2014, pp. 843-849, doi: 10.1109/ICELMACH.2014.6960279.

[10] H. Ouadi, F. Giri, and L. Dugard, "Accounting for magnetic saturation in induction machines modelling," *International Journal of Modelling, Id entification and Control, Inderscience*, vol. 14, no. 1/2, pp. 27-36, 2011, doi: 10.1504/IJMIC.2011.042337.

[11] R. Wamkeue, D. Aguglia, M. Lakehal and P. Viarouge, "Two-step method for identification of nonlinear model of induction machine," *IEEE Transactions on Energy Conversion*, vol. 22, no. 4, pp. 801-809, 2007, doi: 10.1109/TEC.2006.888044.

[12] O. Buchholz, J. Böcker and J. Bonifacio, "Online-identification of the induction machine parameters using the extended kalman filter," *XIII International Conference on Electrical Machines (ICEM)*, 2018, pp. 1623-1629, doi: 10.1109/ICELMACH.2018.8506739.

[13] H. Grotstollen and J. Wiesing, "Torque capability and control of a saturated induction motor over a wide range of flux weakening," *IEEE Transactions on Industrial Electronics*, vol. 42, no. 4, pp. 374-381, 1995, doi: 10.1109/41.402476.

[14] X. Yu, M. W. Dunnigan and B. W. Williams, "A novel rotor resistance identification method for an indirect rotor flux-orientated controlled induction machine system," *IEEE Transactions on Power Electronics*, vol. 17, no. 3, pp. 353-364, 2002, doi: 10.1109/TPEL.2002.1004243.

[15] L. Wang, X. Deng, K. Hu, X. Zhang and K. Wang, "A novel parameter identification method for induction motor," *International Conference on Measuring Technology and Mechatronics Automation*, 2010, pp. 265-268, doi: 10.1109/ICMTMA.2010.20.

[16] P. Vas, "Sensorless vector and direct torque control," Oxford, New York: Oxford University Press, 1998.

[17] A. B. Razzouk, P. Sicard and V. Rajagopalan, "A simple on-line method for rotor resistance updating in indirect rotor flux orientation," *IEEE 2002 28th Annual Conference of the Industrial Electronics Society, IECON 02*, 2002, pp. 317-322 vol.1, doi: 10.1109/IECON.2002.1187528.

[18] A. Ba-Razzouk, A. Cheriti and P. Sicard, "Implementation of a DSP based real-time estimator of induction motors rotor time constant," *IEEE Transactions on Power Electronics*, vol. 17, no. 4, pp. 534-542, 2002, doi: 10.1109/TPEL.2002.800963.

[19] G. V. Pfingsten, S. Steentjes and K. Hameyer, "Operating point resolved loss calculation approach in saturated induction machines," *IEEE Transactions on Industrial Electronics*, vol. 64, no. 3, pp. 2538-2546, 2017, doi: 10.1109/TIE.2016.2597761.

[20] M. Ranta and M. Hinkkanen, "Online identification of parameters defining the saturation characteristics of induction machines," *IEEE Transactions on Industry Applications*, vol. 49, no. 5, pp. 2136-2145, 2013, doi: 10.1109/TIA.2013.2261793.

[21] A. V. Shestakov, "Modeling and experimental analysis of dynamic characteristics of asynchronous motor," *International Conference on Industrial Engineering, Applications and Manufacturing (ICIEAM)*, 2019, pp. 1-4, doi: 10.1109/ICIEAM.2019.8743061.

[22] E. B. Robert, "Modeling and control of synchronous reluctance machines," *Control in Power Electronics*, pp. 251–299, 2002, doi: 10.1016/B978-012402772-5/50009-0.

[23] J. E. Brown, K. P. Kovacs and P. Vas, "A method of including the effects of main flux path saturation in the generalized equations of A.C. machines," *IEEE Transactions on Power Apparatus and Systems*, vol. PAS-102, no. 1, pp. 96-103, 1983, doi: 10.1109/TPAS.1983.318003.

[24] A. Accetta, F. Alonge, M. Cirrincione, M. Pucci and A. Sferlazza, "Feedback linearizing control of induction motor considering magnetic saturation effects," *IEEE Transactions on Industry Applications*, vol. 52, no. 6, pp. 4843-4854, 2016, doi: 10.1109/TIA.2016.2596710.

[25] M. Bertoluzzo, G. S. Buja and R. Menis, "Self-commissioning of RFO IM drives: one-test identification of the magnetization characteristic of the motor," *IEEE Transactions on Industry Applications*, vol. 37, no. 6, pp. 1801-1806, 2001, doi: 10.1109/28.968194.

[26] O. Kiselychnyk, M. Bodson and J. Wang, "Comparison of two magnetic saturation models of induction machines and experimental validation," *IEEE Transactions on Industrial Electronics*, vol. 64, no. 1, pp. 81-90, 2017, doi: 10.1109/TIE.2016.2608766.

[27] M. Chouitek, N. Benouzza, and B. Bekouche, "Control of variable reluctance machine (8/6) by artificiel intelligence techniques," *International Journal of Electrical and Computer Engineering*, vol. 10, no. 2, pp. 1893-1904, 2020, doi: 10.11591/ijece.v10i2.pp1893-1904.

BIOGRAPHIES OF AUTHORS

Mustapha Es-Semyhy 🆔 🇬 SC ⟳ was born in Essaouira, Morocco, in 1989. He is a Ph.D. student. He received his B.Sc. degree in Automation, Automatism and Industrial Informatics from Samlalia Faculty of Science, Cadi Ayad University, in 2014, the M.Sc. degree in Electrical engineering and renewable energy from Science and Technical Faculty, Cadi Ayad University, Marrakesh, Morocco, in 2016.His research interests include adaptive robust nonlinear control of the induction machine and robust nonlinear controller design for PV systems. He can be contacted at email: mustaphaessemyhy@gmail.com.

Abdellfattah Ba-Razzouk 🆔 🇬 SC ⟳ received the Master's degree (M.Sc.A.) in industrial electronics from the Université du Québec à Trois-Rivières (UQTR), Quebec, Canada, in 1993, and the Ph.D. degree in electrical and computer engineering from the École Polytechnique de Montréal, Quebec, Canada, in 1998. From 1997 to 2003, he was a Lecturer in "motors modelling and control" at the Department of Electrical and Computer Engineering, UQTR. In September 1998, he joined the Hydro-Quebec Industrial Research Chair on Power and Electrical Energy, UQTR, where he has been a Professional Research Scientist working on "high-performance intelligent control of electrical drives". Since June 2009, he is a professor in electrical engineering with the Department of Applied Physics and a Researcher affiliated to "Mathematics, Computer and Engineering Sciences Laboratory" and the head of the "Systems Analysis and Information Processing Team", all at the Faculté des Sciences et Techniques, Université Hassan 1er of Settat, Morocco. His research interests include high performance control of adjustable speed drives, parameter identification and adaptive control of electrical motors, neural networks and real-time embedded control systems, renewable energy systems, modelling and computer aided design, and real-time simulation of power electronics systems using multiprocessors platforms. He can be contacted at email: barazzou@yahoo.ca.

Mustapha El Haroussi 🆔 🇬 SC ⟳ was born in Azilal Morocco in 1974; he received his PhD in Error Correcting Codes from Mohammed V University Morocco in 2013. In 2014 he joined, as Professor, applied Physics department of FST, Hassan 1st University, Settat, Morocco. He can be contacted at email: m.elharoussi@gmail.com.

Mhamed Madark 🆔 🇬 SC ⟳ was born in Settat, Morocco, in 1987. He is a Ph.D. doctor. He received his B.Sc. degree in Mathematics Engineering from the Science and Technical Faculty of Hassan 1st University, Settat, Morocco, in 2013; the M.Sc. degree in Automatic, Signal Processing and Industrial Computing from the Science and Technical Faculty of Hassan 1st University, Settat, Morocco, in 2015; and the Ph.D. degree in Automatic, Signal Processing and Industrial Computing engineering from the Science and Technical Faculty of Hassan 1st University, Settat, Morocco, in 2021. His research interests include adaptive robust nonlinear control of the induction machine and robust nosnlinear controller design for three phase grid connected PV systems. He can be contacted at email: m.madark1987@gmail.com.